Published in final edited form as:
Invest Ophthalmol Vis Sci. 2009 August ; 50(8): 3907–3914. doi:10.1167/iovs.08-2448.

Lipofuscin & Autofluorescence Metrics in progressive STGD

R.T. Smith, **N.L. Gomes**, **G. Barile**, **M. Busuioc**, **N. Lee**, and **A. Laine**
Ophthalmology and Biomedical Engineering, Columbia University, New York, NY

Abstract

Purpose—To evaluate Stargardt disease (STGD) progression & relative lipofuscin levels via autofluorescence image analysis.

Methods—We analyzed the relationship between focally increased autofluorescence (FIAF), geographic atrophy (GA) and focally decreased autofluorescence (FDAF) in serial, registered autofluorescence (AF) scans of 10 patients with STGD (20 eyes, 40 scans, mean follow-up 2.0 years) using automated techniques.

Results—GA progressed uniformly in a transition zone with minimal FIAF. Only 4.3% of FIAF progressed to GA or FDAF, despite significant progression of GA (median 30%/yr) and FDAF (mean 29%/yr). As a spatial predictor, the mean chance of FIAF for progression to FDAF was 4.3 ± 4.4%, significantly less than that of random areas (6.7 ± 4.0%, p = 0.029, Mann-Whitney test). For the seven eyes with GA, the mean chance of FIAF in the transition zone for transition to GA was 12 ± 8.9%, significantly less than that of random areas (33 ± 3.6%, p = 0.026, Mann-Whitney test).

Conclusions—Autofluorescent flecks and FIAF deposits with AF levels elevated above the *initial* macular background were less likely in the short term (2 years) to transform to GA and FDAF (AF levels below the *final* background) than random areas, suggesting additional mechanisms beyond direct lipofuscin toxicity. FIAF/FDAF levels were observed to fluctuate, with focal remodeling of FIAF and FDAF, or rarely, even transition of FDAF to FIAF. FDAF tended to develop, not coincident with, but adjacent to initial FIAF. Because AF identifies these characteristic biologic markers so specifically, autofluorescence metrics merit consideration in the study of Stargardt disease.

Introduction

There is considerable interest in the effect of lipofuscin on retinal pigment epithelium (RPE) function and its role in retinal diseases. Lipofuscin granules accumulate with age in postmitotic RPE lysosomal compartments as phagocytotic remnants of photoreceptor outer segment discs.[1-5] Previous studies suggest that lipofuscin and its constituent A2E may exert toxic effects on normal RPE cellular processes.[6-11]

Lipofuscin granules also accumulate more rapidly than with normal aging in monogenic retinal disorders, such as Best disease and Stargardt disease, and complex degenerative diseases such as age-related macular degeneration (AMD).[8,12,13] However, the precise influence of these granules remains uncertain.

Lipofuscin accumulation has been examined in vivo with fundus autofluorescence (FAF) using confocal scanning laser ophthalmoscopy. A number of studies demonstrate that hyperfluorescent FAF signals are reliable markers of lipofuscin in RPE cells.[14-17]

Abnormal lipofuscin accumulation may occur in the junctional zones of geographic atrophy (GA) in AMD.[16] The importance of this phenomenon remains unclear. A previous study based on a small case series of three eyes suggested that areas of increased FAF may predict development or enlargement of geographic atrophy.[18] A subsequent study of eight eyes

which used image analysis for precise localization of FIAF and subsequent development of new GA, however, found the predictive value of FIAF approximately the same as chance. [19] It has also been asserted that areas without FIAF will not progress to GA, i.e., that lack of FIAF has a negative predictive value for development of GA. [18] However, the same subsequent study did not confirm this.[19] More generally, the use of multimodal image registration and digital analysis of lesion co-localization can provide rigorous quantitative testing of hypotheses initially based on qualitative observations.[20]

The view that excess lipofuscin is the driving force for RPE cell death in STGD is also widely held, even though it is recognized that some STGD patients have normal or low levels of lipofuscin compared to normal age-matched controls (Lois et al). [21] This is partly explained in this paper by duration of disease, with longer duration associated with lower AF levels and the examples with lower AF in turn mostly associated with central atrophy. However, there were examples without atrophy and fairly similar 2D AF scans, but very different AF levels (normal to high). Thus, although there was a general trend for more atrophy and decreasing AF with time, outside areas of frank atrophy, absolute AF levels could vary widely. The goal of this study is therefore to use our digital techniques to determine whether lipofuscin accumulation in *relative* excess above background levels, as measured by FIAF, is a direct spatial precursor for GA progression or for the development of focally decreased (*relative* to background levels) autofluorescence (FDAF) in a two year time frame. This will be achieved by analyzing serial AF images in STGD patients for the spatial relationship of FIAF in the initial images to new GA and new FDAF in the final images.

Subjects and Methods

Patient Selection and Image Acquisition

Images of 20 eyes from 10 patients with STGD were selected retrospectively from a database of patients imaged from 2002 to 2008 at the Columbia University. All patients had STGD by ABCA4 genotyping. Each eye had an initial and a final AF image (40 total images, mean follow-up 2.0 years). FIAF and FDAF were present in all eyes. GA was present in 7 eyes. The ages of the patients ranged from 6 to 57 years (mean age 34 years). The age of onset, mean 27 years, was defined as the age at which visual loss was first noted. The dataset included 4 males and 6 females, 9 Caucasians and 1 Asian.

After pupillary dilation, fundus AF images had been recorded using the Heidelberg model HRA or HRA2 confocal SLO (Heidelberg Inc, Heidelberg, DE). This instrument uses blue laser light at 488 nm for illumination and a barrier filter at 500 nm to limit the captured light to autofluorescent structures. The AF images consisted of bitmapped laser scans centered on the macula. Each image was an average of 3 to 6 scans composed by the SLO software. We required good quality (second order vascular branches definable throughout the macula) in both the initial and final images so that FAF abnormalities would be well-characterized.

The initial and final AF images were registered in Matlab R2006 (The Mathworks, Inc., Natick, Massachusetts). We tested accuracy by superimposing the two images in Adobe Photoshop CS2 as a layered image (Adobe Systems Inc., San Jose, CA) and flickering one of them on and off. The constant features are the retinal vasculature, and corresponding vessels should remain stationary. If registration was inaccurate, a new registration was performed by picking additional vascular landmarks in the Matlab program, and continuing until the result was satisfactory. Because they were precisely superimposed, both image scales were identical and exact spatial relations between FAF abnormalities in the initial and final images could be determined. The image pair was then cropped to a square including the fovea. All subsequent analysis was done on these images.

The study followed the tenets of the Declaration of Helsinki and received approval by the institutional review board of New York Presbyterian Hospital, New York, NY.

Image Analysis

In order to make quantitative assessments of FIAF and FDAF relative to the image background in the presence of significant background variability, the AF image was leveled with a 12 zone quadratic polynomial mathematical model of the background in the manner previously described for AF images in AMD. [19] The mathematical model for leveling the background also includes a luteal compensation by a Gaussian distribution for subjects in which the fovea is not completely atrophic. It uses published data on the spatial distribution of macular pigment and is described in more detail in an earlier paper in the context of fundus photography, but the concept is the same[22]. The math model of the *background* also specifically excludes hyperautofluorescent pixels as input: In each of the 12 zones, areas of FIAF are located by the two threshold, three class Otsu method and removed from the background pixels used as input to the model. This ensures that bright non-background pixel values do not artificially elevate the model in their vicinity. (For details see Hwang et al, [19], p. 2656).

When GA was present, it was segmented separately before leveling the remainder of the image with the model. The definition of GA included the criteria of being large (> 150 microns in size), homogeneous and well demarcated areas of profound hypoautofluorescence (gray levels within three gray scale values of those found in the disc) to distinguish it from small areas of less profound hypoautofluorescence, which then were defined as focally decreased autofluorescence (FDAF) if they met the following criterion. Briefly, after masking any GA and leveling the background, the mean and standard deviation σ of the resulting leveled image were used to define the thresholds for increased FAF and decreased FAF. These thresholds were set at 1.5 σ above and below the mean, respectively, to determine the total FIAF and FDAF in the image.

The choice of 1.5 σ was empiric, because we found that it gave the best selection of visually evident abnormalities in the STGD images. The imposition of a single threshold also lent some objectivity to an otherwise very subjective task. However, we recognize that that no single method or threshold can be the final arbiter of abnormality versus normality. For this reason, a sensitivity analysis was also conducted to measure the impact of redefining FIAF/FDAF thresholds at 1.0 and 2.0 σ above/below the mean in four patients. Indeed, there is no currently agreed upon standard for AF abnormalities, Thus, when abnormalities were clearly present to visual inspection, the purpose of the method was to identify them efficiently so that the scientist did not spend countless tedious hours drawing them by hand for further analysis. However, manual intervention was still sometimes necessary. For example, vessel fragments were often incorrectly identified as FDAF by the basic threshold. These were removed partly by morphologic criteria in the automated system, but also manually in some cases. The morphologic criteria enabled in Matlab were based on two observations: 1. Single vessel fragments were usually much more eccentric than FDAF lesions. 2. However, vessel fragments with bifurcations were not necessarily eccentric. Therefore: 1. All FDAF connected components with eccentricity greater than 0.975 were removed. 2. Remaining connected components were skeletonized and bifurcation points removed. The separated components were retested and highly eccentric components were removed as before. The remaining segments and bifurcation points were reconstructed and retested to complete the analysis. These highly conservative criteria resulted in most vessel fragments being removed, but rarely any FDAF lesion. Remaining corrections were performed manually. Further optimization of this portion of the algorithm could have been done, but was beyond the scope required for this paper.

There is also the interesting question of what happens when the method is applied to a normal image. It obviously makes no sense to insist there are “abnormal areas” in a normal scan! The answer lies in our earlier publication in which the mathematical model was first introduced and validated on normal AF [19] The fact that the model is accurate to within the noise levels for normal images was demonstrated in detail in this paper on the relation of FIAF and GA in AMD. Put another way, for normal images, as in the figure in [19], the method basically identifies noise in the image (and vessels for FDAF) rather than abnormalities. Precisely, we found that 99.7% of pixels in the leveled image (other than vessels) fell within 2.0 σ of the mean in each. Thus, only tiny fractions of pixels, on the order of 0.3%, would be identified as abnormal by this criterion. No particular change with age was noted in this normal population, ages ranging from 32 to 58. By contrast, if the gray levels of the image had a normal distribution, then gray levels above 2.0 σ would comprise 2.3% of the image.

For each pair of registered images, a region of interest (ROI) was defined that included all significant FIAF and new FDAF. Because the areas of FDAF were variably scattered in the different images, a ROI was used in a non-standardized but intuitively obvious manner (see Fig 1). Calculations of lesion areas and predictive values of FIAF were all made with reference to this ROI where the disease activity of interest resided. In those cases in which actual GA was also present, the 250 micrometer border zone around the GA was taken as a separate ROI just as for GA in an AMD image, and separate calculations of the predictive values of FIAF for new GA formation were performed with respect to this region. New dark pixels at the edge of established GA were classed as new GA, but otherwise were classified as new FDAF. Thus, we studied two classes of dark regions on each AF scan: GA and FDAF, and the predictive values of FIAF were calculated separately for each of these two classes.

Measurements

All areas of FIAF in the original image, and new FDAF and new GA in the final image, were expressed as percentages of the ROI, e.g., p(FIAF) = 3.2%. Those pixels of FIAF in the original image that overlay new FDAF in the final image (in the registered image pair) were denoted by the intersection FIAF ∩ NewFDAF. As described previously for the case of GA[19], the positive predictive value (PPV) that pixels with increased FAF would become new FDAF was given by:

$$PPV\_FIAF = \frac{p(FIAF \cap NewFDAF)}{p(FIAF)} X100\%$$

Thus, this was the percentage probability that any pixel with increased FAF in the initial image became part of new FDAF in the final image. Note that in this setting we have adopted the term positive predictive value as a convenient nomenclature to compare the observed results in our patients to theoretical results that would hold if all FIAF turned to FDAF in the period of observation. Obviously, the theoretic result was not expected, but did provide a standard for comparing the behavior of other areas of the macula when *both* were measured by the same standard.

The probability that any pixel in the original image falls by random chance alone into new FDAF is equal to the area of new FDAF, or p(newFDAF). That is, the PPV of random guessing is exactly as good as the percentage area of new FDAF:

$$PPV\_Chance = p(newFDAF).$$

The negative predictive value (NPV) of increased FAF, i.e. that pixels *without* increased FAF (denoted ~ FIAF) would *not* become atrophic (denoted ~newFDAF), was given by:

$$NPV\_FIAF = \frac{p(\sim FIAF \cap \sim NewFDAF)}{p(\sim FIAF)} X100\%$$

This is the probability that any pixel without increased FAF in the initial image did not develop FDAF in the final image. The negative predictive value of chance, i.e., that a randomly chosen pixel does *not* fall into new FDAF, is exactly the percentage of the region that is not newFDAF:

$$NPV\_Chance = 100\% \;\; p(NewFDAF).$$

Note in summary that while the image analysis method evaluated each image on a pixel basis, the measurements in this section were always in terms of total areas, or ratios of total areas, of pixels in the various categories. Thus, for each eye, all observations on a pixel basis were aggregated, first into relevant areas of FIAF, etc, and then ratios to determine the PPV, etc., as single numbers. These single numbers were the outcome variables that were compared in the results, and individual pixels were no longer considered. Hence, the approach was to try to describe complex phenomena occurring throughout the macula in simple terms by single numbers. Also, in aggregating observations based on large numbers of pixels, rather than individual pixels or small lesions, the effects of noise were more likely to average out.

The predictive values of FIAF for the development of new GA were all defined analogously: precisely, in each equation, new FDAF is replaced by new GA. For a more complete discussion of the GA case, see Hwang et al.[19] In the case where both GA and FDAF were present, we calculated the probabilities for FIAF to transform into new GA or new FDAF separately.

Total quantities of FIAF and FDAF were also measured in each image, and the yearly rate of change in serial image pairs was calculated. For brevity in discussion we refer to decreasing FIAF or increasing FDAF or GA, either locally or globally, as a “decreasing AF” transition, with the understanding that all quantities are relative to the AF background. Likewise, increasing FIAF or decreasing FDAF is termed an “increasing AF” transition. Note that when total measured FIAF is decreasing, either the background (absolute) AF is increasing and/or the (absolute) AF in the flecks is decreasing, which in turn may depend on the stage of the disease. Similarly, when total FDAF is increasing, either the background (absolute) AF is increasing and/or the (absolute) AF in FDAF areas is decreasing

Results

Progression and remodeling of FDAF/FIAF

While the long term trend was for decreasing AF overall, focally increased and decreased AF were observed to be in a constant process of remodeling, with these lesions interchanging position and intensity (Figs 1 and 3). Bright flecks did not necessarily turn dark, but often simply faded. Unexpectedly, even FDAF lesions were observed to turn bright in five patients (Fig 3). Indeed, the total amount of FIAF and FDAF could change , in either direction. Thus, while the mean rates of change were mostly in the decreasing AF direction (for FDAF 30 ± 45%/yr, range -51% to +147%/yr; for FIAF -16 ± 35%/yr, range -91% to +65%/yr), the range in each case included several examples of increasing AF (Table 1). Individual cases still need to be interpreted with care for the relative nature of the measurements. For example, the large drop in detected FIAF (- 43% OD) in 7 year old patient #6 (Table 1) could have been caused

by a generalized *rise* in background AF in this young rapid progressor, resulting in fewer areas of distinctly elevated AF. GA lesions of course remained atrophic, and the area of GA could only increase.

Predictive power of FIAF for new FDAF and new GA

As mentioned in Methods, the population being studied for purposes of the final statistical comparisons was not the population of pixels in a given eye, but rather the study population of 20 eyes. Thus, one set of observations was the set of 20 measurements of PPV for FIAF; another was the set of measurements of PPV for chance, etc. In these eyes over a median period of 2.0 years, the mean positive predictive power of focally increased autofluorescence for transition to focally decreased autofluorescence was 4.3 ± 4.4%, significantly less than that of random pixel selection (6.7 ± 4.0%, $p = 0.029$, Mann-Whitney test). The mean negative predictive power of FIAF for transition to FDAF was 93 ± 4.0%, the same as that of chance (93 ± 4.0%, NS, Table 1).

For the seven eyes with GA, the mean chance of FIAF in the transition zone for transition to GA was 12 ± 8.9%, significantly less than that of random areas (33 ± 3.6%, $p = 0.026$, Mann-Whitney test). The mean negative predictive power of FIAF for transition to GA was 67 ± 3.5%, the same as that of chance (67 ± 3.6%, NS, Table 2). Only one eye (Patient 10, OD) had a positive predictive value of FIAF for new GA greater than chance. For each of the other six eyes with GA, this value was substantially less than chance (Table 2).

Age of onset and duration of disease are presented in Table 1. Although there is as expected fading of flecks and increasing FDAF or even atrophy later in the disease course, the findings, however, remained unchanged when age and duration were considered. Specifically, the PPV of FIAF remained less than that of chance for age above or below the mean, for duration of disease above or below the mean, and in the presence or absence of atrophy. That is, the PPV of FIAF remained less than that of chance in these six subgroups: age > 34 (6.7% vs. 3.9%), age<34 (6.5% vs. 4.9%); duration of disease > 7 years (8.5% vs. 5.1%), duration of disease < 7 years (5.2% vs. 3.0%); eyes with atrophy (7.7% vs. 4.9%) and eyes without atrophy (6.2% vs. 3.4%).

There was no correlation between total initial FIAF load and subsequent rate of total GA or FDAF progression (Tables 1, 2).

Sensitivity of predictive power to definition of FIAF

Increased and decreased FAF were empirically defined to be 1.5 standard deviations above/below the mean image intensity in the leveled image. To consider the possibility that another definition could have changed the calculated predictive values, a sample set of calculations in four sets of serial images in which increased FAF was defined as 1.0 or 2.0 standard deviations above the mean was performed. It gave no systematic improvement in positive predictive values for FDAF. Two of the eight new values were better than chance, and the rest were near or below chance (Table 3). A similar calculation for the *only* eye with GA and a PPV for FIAF and GA greater than chance (Patient 10 OD, Table 3) showed slight improvement for sigma = 2.0 and no change for sigma = 1.0.

The GA transition zone

For the seven eyes with GA, as a fraction of the 250 micrometer border zone, the mean new GA was 33 ± 4%, and GA progressed at a median yearly rate of 30%/yr with respect to baseline. However, these transition zones generally had minimal FIAF (mean 3 ± 1%) and displayed one of three qualitative AF types: a neutral AF level, with patches of minimally elevated and decreased AF as in Fig 2 (four eyes); predominantly FDAF (two eyes of two patients); and

mixed patches of FIAF/FDAF (one eye). Only the last eye had significant FIAF in the transition zone. An example of each of the three types is presented in Fig 4.

Discussion

The relationships between FIAF, FDAF and GA in active STGD appear to be complex and in this study did not follow a consistent or monotonic progression either from FIAF to FDAF or from FIAF to GA as might be expected from direct lipofuscin toxicity. Total FIAF levels did not always decrease, nor did FDAF quantities always increase, as generally supposed, but could fluctuate for a period, with focal remodeling of FIAF and FDAF, or rarely, even focal transition of FDAF to FIAF. There was a striking tendency for FDAF to develop, not coincident with, but adjacent to initial FIAF.

The appearance of increasing FIAF could simply be explained by the stage of disease activity which was captured by the serial images. In active disease, more lipofuscin could be being produced and imaged as flecks with time. It is more difficult to explain decreasing total FDAF on a cellular basis. It is unlikely that diseased cells headed to apoptosis, which were already low on lipofuscin, somehow managed to regain lipofuscin. Instead, perhaps there is a mechanism of local remodeling of the RPE layer that results in adjacent confluent areas of thickening and thinning. If the number of lipofuscin granules stays constant during changes in cell shape, they could be more tightly packed in the axis of autofluorescence visualization, resulting in FIAF, and more widely dispersed in that same axis, resulting in FDAF. Such a mechanism is consistent with the observations of this study.

The transition zones for areas of GA in our seven cases fell into three recognizable types, only one case of which contained significant FIAF. This is contrary to AMD, in which there is often significant FIAF in the border zone[18,19]. Qualitatively, these types differ mostly in overall fluorescence levels, and may just represent different stages in the same process (Fig 4).

Quantitative analysis of these phenomena also provided unexpected findings. While qualitative study certainly showed the variability of lesion expression and relationships, one might still have expected that the majority of lesion transformations would display decreasing AF transitions. To test this hypothesis, precise registration of serial images, coupled with automated identification of lesion types in the original and final images, allowed computation of correlations not feasible by manual methods or visual inspection. These data, however, did more than suggest a mere lack of association between focal lipofuscin deposits as imaged by AF and subsequent RPE damage (loss of lipofuscin) as evidenced by focally decreased AF and GA. The mean predictive values for FIAF, significantly less than that of chance, suggest that initial FIAF and subsequent FDAF tend to *avoid* coinciding. The qualitative spatial relationships, as illustrated in Figs 1 and 3 and as we commonly observed, were consistent with these calculations and further demonstrated a striking tendency for these lesions, while avoiding coincidence, to occur *adjacent* to one another. The biological implications are unclear. For example, if lipofuscin and/or melanolipofuscin were accumulating *next to* RPE that was undergoing damage and losing lipofuscin, perhaps the later appearance of hypoautofluorescent RPE adjacent to such lipofuscin deposits could be explained. This sequence would parallel that noted in our previous study of AF and drusen in AMD, in which FIAF at first co-localized with drusen in early AMD and then was found adjacent to drusen and GA as atrophy supervened [20].

The study has several limitations:

1. This is a retrospective study of 20 eyes in 10 patients, which may not be representative of the phenotypically heterogeneous STGD population and could reflect some selection bias. Also, successive (days or weeks) imaging was not a possibility in this

retrospective study to assess reproducibility of measurements. Noise and image acquisition variability produce image variation in successive AF images. However, an advantage of the method is that by leveling the background, acquisition illumination variability is largely eliminated (see figures). Additionally, with the good quality scans used in this study, the key abnormalities were visually evident and detected by the method.

2. Images were derived from the HRA/HRA2 software, which registers and averages multiple individual AF scans. In each case, the number of scans averaged may differ due to scan quality and availability, resulting in differences in image dynamic range and signal-to-noise ratio. The resulting images also therefore report relative AF levels, not absolute levels. To acquire absolute levels would require spectrophotometric measurements on a point by point basis as was done in the seminal studies by Delori [14,15]. Thus, this study describes the relationship between relative levels; precisely, between (relatively) elevated AF levels in the original image to (relatively) decreased levels in the final image. We cannot know if an area of 'normal background AF' on a given STGD patient image actually has normal lipofuscin content, or perhaps higher, or even lower lipofuscin content than a normal control[21]. Bright flecks are thus simply focal areas of higher lipofuscin concentration than background levels. However, if lipofuscin were toxic, one logical prediction would still be for a dose-response in which bright flecks were more likely than random areas to turn dark in time. The finding herein, albeit for an average interval of only 2 years in this chronic disease, was that bright flecks were statistically significantly *less* likely than random spots to turn dark. This pattern was maintained even in our patient with 5 year follow-up, (Patient 8, Fig 3).

3. As stated, the limited follow up time is a limitation. What might happen in 5 years of observation is of course speculation. However, one might argue, for example, that additional areas of FIAF would transition to GA, thus giving an increased positive predictive value for FIAF at this point and bolstering a conclusion that FIAF predicts GA after all. However, note that *all* measurements would have to be redone at the 5 year point. As GA progresses, the PPV for chance (which is simply the fractional area of new GA) increases also. We must also posit that that the PPV of FIAF starts out less than that of chance at the two year point, because this is shown by the present study. A moment's reflection now makes it clear that if the PPV of FIAF starts out *behind* that of chance, it is not sufficient that more FIAF simply turns to GA with time to return to a conclusion that FIAF predicts GA. The trend would have to significantly *reverse* with time for FIAF to catch up or pass the predictive value of chance, which is *always* increasing. The point here is to emphasize that even "obvious" conclusions based on reasonable speculation about past or future events may be incorrect. Further follow-up with real data should resolve some of these questions.

4. Another concern might be whether a median 2 year time interval is sufficient to detect significant changes in any case. But as just noted in the Results, the mean annual rates of change of FIAF and FDAF area were both significant (-16% and +30%, respectively), and GA area progressed at a substantial annual median of 30% also. For example, Fig. 2 demonstrates significant enlargement in two years of central GA into a border zone without FIAF. Fig. 3 shows marked fading of flecks over two years, with appearance of many more areas of FDAF, which, however, did not correspond to the original flecks.

5. Increased and decreased FAF were empirically defined to be 1.5 standard deviations above/below the mean image intensity in the leveled image. However, we also considered more or less bright populations of flecks, as determined by standard deviations above the mean, to see if greater or less lipofuscin content affected

predictive values significantly (Table 3). It did not, bolstering the basic conclusions of the study, and also providing further evidence against a dose-response for lipofuscin load.

A main strength of the study is the quantitative rather than qualitative nature of the analysis and conclusions. Another is the uniformity of the findings across 20 eyes of 10 patients: not only were the conclusions statistically significant, but each individual eye also showed little sign of FIAF turning to FDAF or GA

In conclusion, autofluorescent flecks and FIAF deposits with AF levels elevated above the macular background level were less likely in the short term (2 years) to transform to Stargardt disease manifestations of GA and focally decreased AF than randomly chosen areas, suggesting a multifactorial and/or time delayed pathogenesis with RPE damage mediated in part through non-fluorescent intermediates or other mechanisms. Further study over a longer period of observation is warranted of the complex time course and relationships of FIAF, FDAF and GA, which in turn may offer further insight on the biology of this disease. Advances in AF imaging in the future may also offer data on absolute rather than relative lipofuscin levels, thus allowing AF image analysis to be more definitive about the role of lipofuscin.

Because AF identifies lipofuscin accumulation and GA so specifically, and because these are the most characteristic biologic markers of STGD, autofluorescence metrics in STGD merit consideration in the study and eventual therapy of this disease.

References

1. Feeney-Burns L, Berman ER, Rothman H. Lipofuscin of human retinal pigment epithelium. American Journal of Ophthalmology 1980;90(6):783–91. [PubMed: 7446665]
2. Katz ML, Gao CL, Rice LM. Formation of lipofuscin-like fluorophores by reaction of retinal with photoreceptor outer segments and liposomes. Mechanisms of Ageing & Development 1996;92(23): 159–74. [PubMed: 9080396]
3. Kennedy CJ, Rakoczy PE, Constable IJ. Lipofuscin of the retinal pigment epithelium: a review. Eye 1995;9(Pt 6):763–71. [PubMed: 8849547]
4. Weiter JJ, et al. Retinal pigment epithelial lipofuscin and melanin and choroidal melanin in human eyes. Investigative Ophthalmology & Visual Science 1986;27(2):145–52. [PubMed: 3943941]
5. Sparrow JR, Boulton M. RPE lipofuscin and its role in retinal pathobiology. Experimental Eye Research 2005;80(5):595–606. [PubMed: 15862166]
6. Boulton M, et al. The formation of autofluorescent granules in cultured human RPE. Investigative Ophthalmology & Visual Science 1989;30(1):82–9. [PubMed: 2912915]
7. Young RW. Pathophysiology of age-related macular degeneration. Survey of Ophthalmology 1987;31 (5):291–306. [PubMed: 3299827]
8. Dorey CK, et al. Cell loss in the aging retina. Relationship to lipofuscin accumulation and macular degeneration. Investigative Ophthalmology & Visual Science 1989;30(8):1691–9. [PubMed: 2759786]
9. Holz FG, et al. Inhibition of lysosomal degradative functions in RPE cells by a retinoid component of lipofuscin. Investigative Ophthalmology & Visual Science 1999;40(3):737–43. [PubMed: 10067978]
10. Zhou J, et al. Mechanisms for the induction of HNE- MDA- and AGE-adducts, RAGE and VEGF in retinal pigment epithelial cells. Experimental Eye Research 2005;80(4):567–80. [PubMed: 15781285]
11. Sparrow J, et al. A2E, a byproduct of the visual cycle. Vision Research 2003;43(28):2983–90. [PubMed: 14611934]
12. Frangieh GT, Green WR, Fine SL. A histopathologic study of Best's macular dystrophy. Archives of Ophthalmology 1982;100(7):1115–21. [PubMed: 7092655]
13. O'Gorman S, et al. Histopathologic findings in Best's vitelliform macular dystrophy. Archives of Ophthalmology 1988;106(9):1261–8. [PubMed: 3415551]

14. Delori FC, et al. Autofluorescence distribution associated with drusen in age-related macular degeneration. Investigative Ophthalmology & Visual Science 2000;41(2):496–504. [PubMed: 10670481]

15. Delori FC, et al. In vivo fluorescence of the ocular fundus exhibits retinal pigment epithelium lipofuscin characteristics. Investigative Ophthalmology & Visual Science 1995;36(3):718–29. [PubMed: 7890502]

16. von Ruckmann A, Fitzke FW, Bird AC. Fundus autofluorescence in age-related macular disease imaged with a laser scanning ophthalmoscope. Investigative Ophthalmology & Visual Science 1997;38(2):478–86. [PubMed: 9040481]

17. von Ruckmann A, Fitzke FW, Bird AC. Distribution of fundus autofluorescence with a scanning laser ophthalmoscope. British Journal of Ophthalmology 1995;79(5):407–12. [PubMed: 7612549] comment

18. Holz FG, et al. Fundus autofluorescence and development of geographic atrophy in age-related macular degeneration. Investigative Ophthalmology & Visual Science 2001;42(5):1051–6. [PubMed: 11274085]

19. Hwang JC, et al. Predictive value of fundus autofluorescence for development of geographic atrophy in age-related macular degeneration. Investigative Ophthalmology & Visual Science 2006;47(6): 2655–61. [PubMed: 16723483]

20. Smith RT, et al. Autofluorescence characteristics of early, atrophic, and high-risk fellow eyes in age-related macular degeneration. Investigative Ophthalmology & Visual Science 2006;47(12):5495–504. [PubMed: 17122141]

21. Lois N, et al. Fundus autofluorescence in Stargardt macular dystrophy-fundus flavimaculatus. American Journal of Ophthalmology 2004;138(1):55–63. [PubMed: 15234282]

22. Smith RT, et al. A method of drusen measurement based on the geometry of fundus reflectance. BioMedical Engineering OnLine 2003;2:10. [PubMed: 12740042]

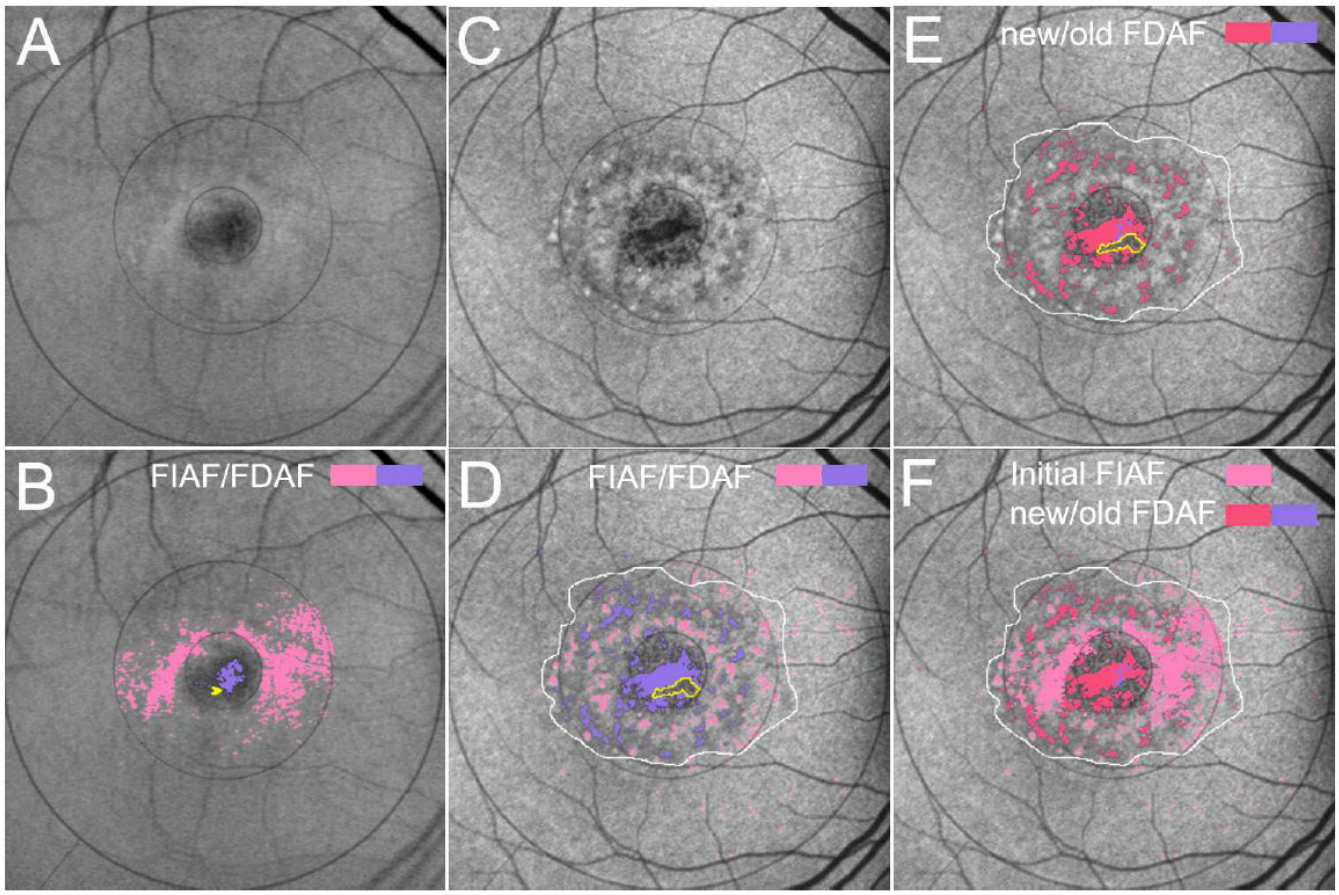

Fig 1. Patient 8. OD. 5 year progression and remodeling of focally decreased autofluorescence

A. AF image 2002, original. **B**. focally increased autofluorescence (FIAF) and focally decreased autofluorescence (FDAF) detected by the model in **A**. The "ghost vessels" in the 2002 image (but not present in 2007) are an artifact caused by misalignment of one of the raw images used to generate the 2002 scan, The vessels in that image are thus faintly perceived. These "ghosts" did not affect the segmentation. **C**. AF image 2007, original, registered to the image from 2002. **D**. FIAF and FDAF detected by the model in **C**. The white ring is the region of interest (ROI) that included all significant FIAF and new FDAF. The FDAF is larger by a factor of 7 in area since 2002. Both FIAF and FDAF are more scattered and peripheral in the later image. However, there is also remodeling of the FDAF centrally. Note in particular the yellow outlined area in D, which is an island of mottled but not decreased autofluorescence within the larger new area of FDAF. If we locate this island, just below the foveal center, in the initial images in **B**, we see that it formerly contained some decreased autofluorescence that is now no longer decreased (yellow arrowhead) **E**. FDAF is divided into new (not present in 2002) and old (present in 2002). We clearly see old FDAF (purple) within the yellow outlined island that has now returned to normal AF levels. **F**. To see the relation of AF levels to new FDAF formation, the FIAF from 2002 is overlaid on the new FDAF in 2007 New FDAF arises both inside and outside the initial FIAF ring, but little coincides. Despite significant increase in area of FDAF, only 4.8% of FIAF pixels turn to FDAF in 5 years, relative to 7.1%. of randomly chosen pixels, New FDAF appears *adjacent* to initial FIAF but is not *coincident* with it: an FIAF lesion is *less* likely to turn to FDAF than another randomly chosen point.

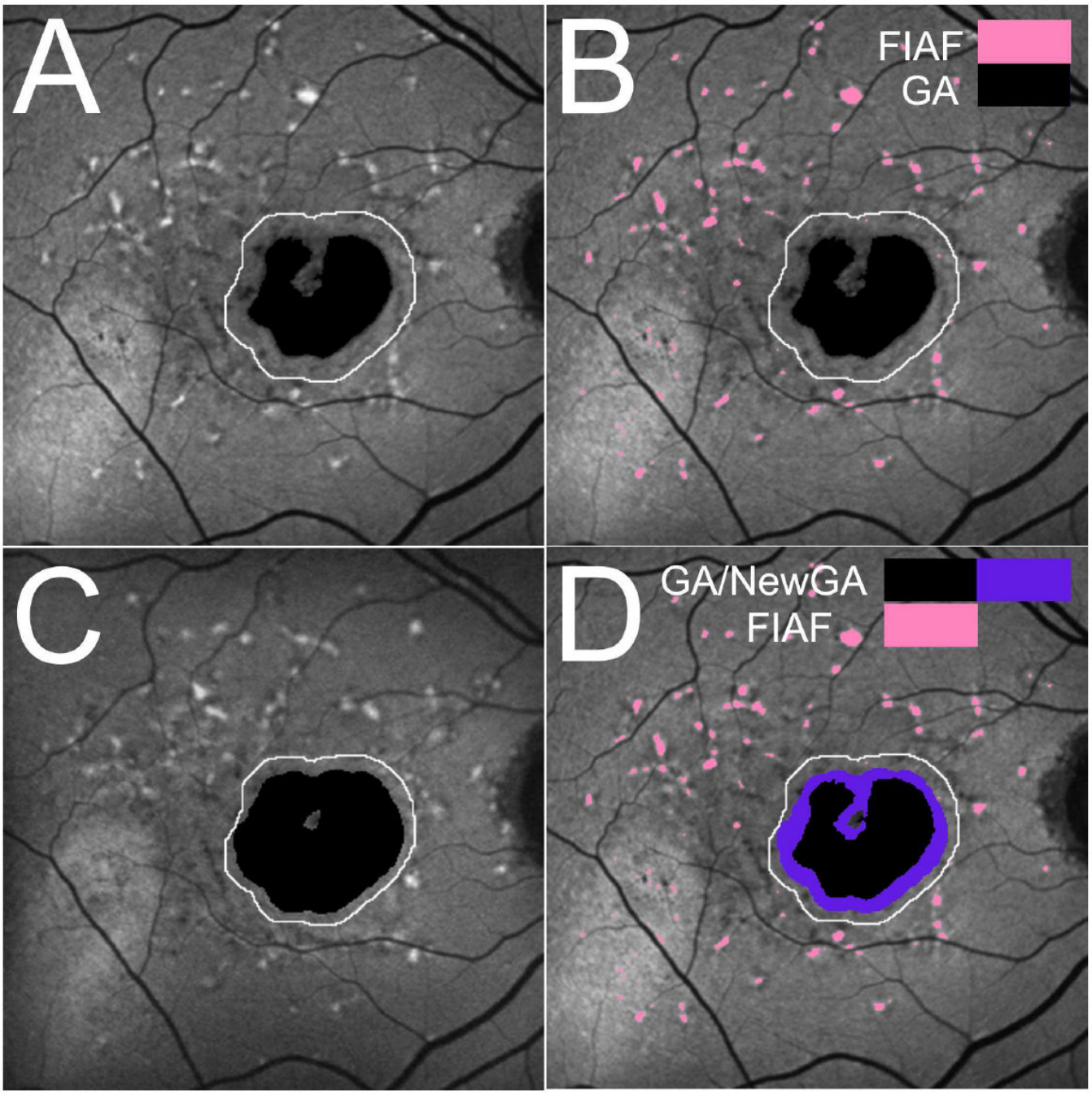

Fig 2. Patient 2 OD. 2 year progression of geographic atrophy in 53 y/o male

A. Initial AF scan, 2006, with 250 μ border zone in outlined in white. **B**. Geographic atrophy (GA) segmented in black and focally increased autofluorescence (FIAF) in pink, mostly outside the border zone. The border zone itself has neither significant FIAF nor focally decreased autofluorescence (FDAF), but does have patches of minimally elevated and decreased AF. **C**. Final AF scan, 2008, registered exactly to 2006 scan, with same border zone superimposed. The GA has progressed. **D**. Superimposition of the final GA from **C** on the initial GA in **B** allows identification of the new GA (dark violet). It has grown significantly, uniformly in all directions, and is also essentially unrelated to the initial FIAF. In fact, there are only two tiny FIAF pixels in the border zone, and neither turns to GA (predictive value of 0).

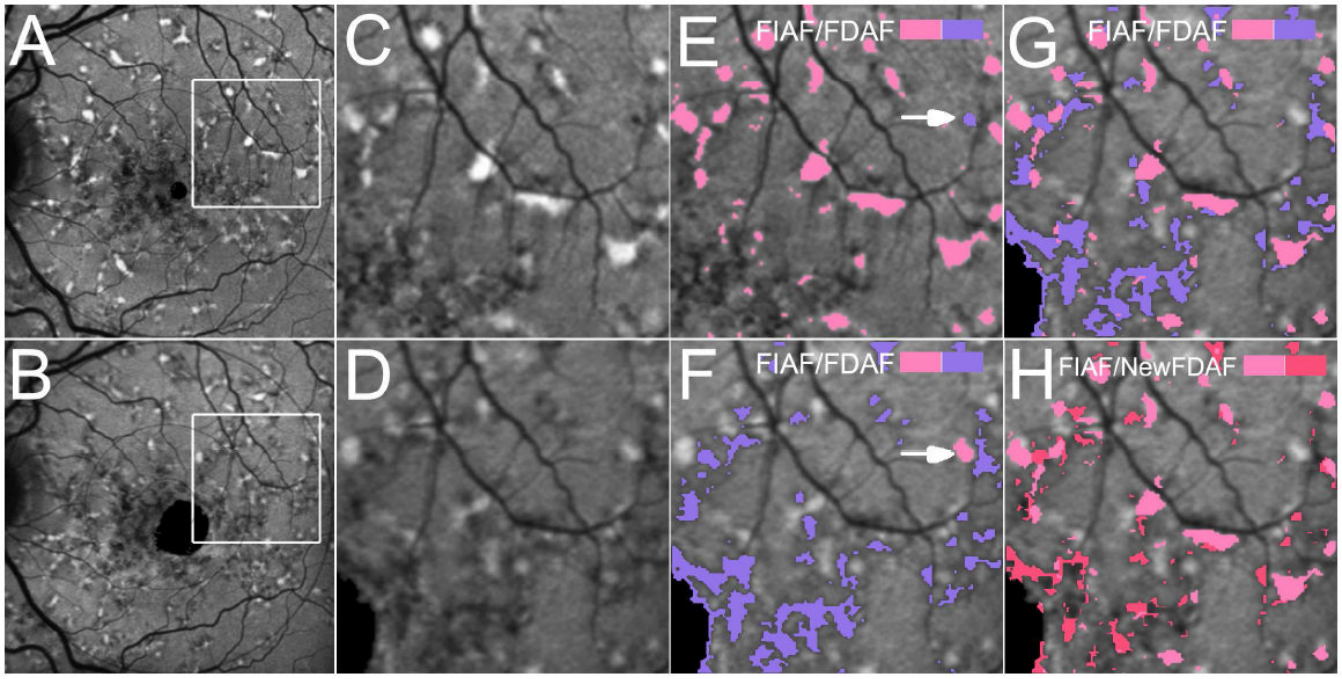

Fig 3. Patient 10 OS. Local relationships of focally increased autofluorescence and new focally decreased autofluorescence over 2 years

This series shows a typical progression in the totals of focally increased autofluorescence (FIAF) and focally decreased autofluorescence (FDAF) over two years. **A**. Initial image, original. **B**. Final image, registered to initial image. On qualitative inspection of the original images, there appear to be fewer flecks of FIAF and more areas of FDAF in the final compared to the initial image. Precisely, after automated detection, this impression was confirmed: the area of FDAF was found to have increased 14% and the area of FIAF decreased 52% overall. The geographic atrophy (GA) has increased dramatically, by a factor of 10. The same is true for the regions enclosed in the white square: **C**, initial image, **D**, final image, where the area of FDAF has increased 26% and the area of FIAF has decreased 50%. GA is present in the final image, but not in the initial. **E**. The FIAF in the initial image is segmented in pink. **F**. The FDAF in the final image is segmented in violet. Despite the general trend to decreasing FIAF, a single FDAF lesion in the *initial* image, **E**, white arrow, has also been selected to illustrate increasing AF transformation to a single FIAF lesion in the *final* image, **F**, white arrow. The detailed relationship between the initial FIAF and final FDAF is illustrated in **G**, with the FIAF from **E** superimposed on the FDAF in **F**. It is remarkable how very closely *adjacent* many of these lesions are, without actually coinciding. This relationship still holds in **H**, when only new FDAF, red, is juxtaposed with the initial FIAF.

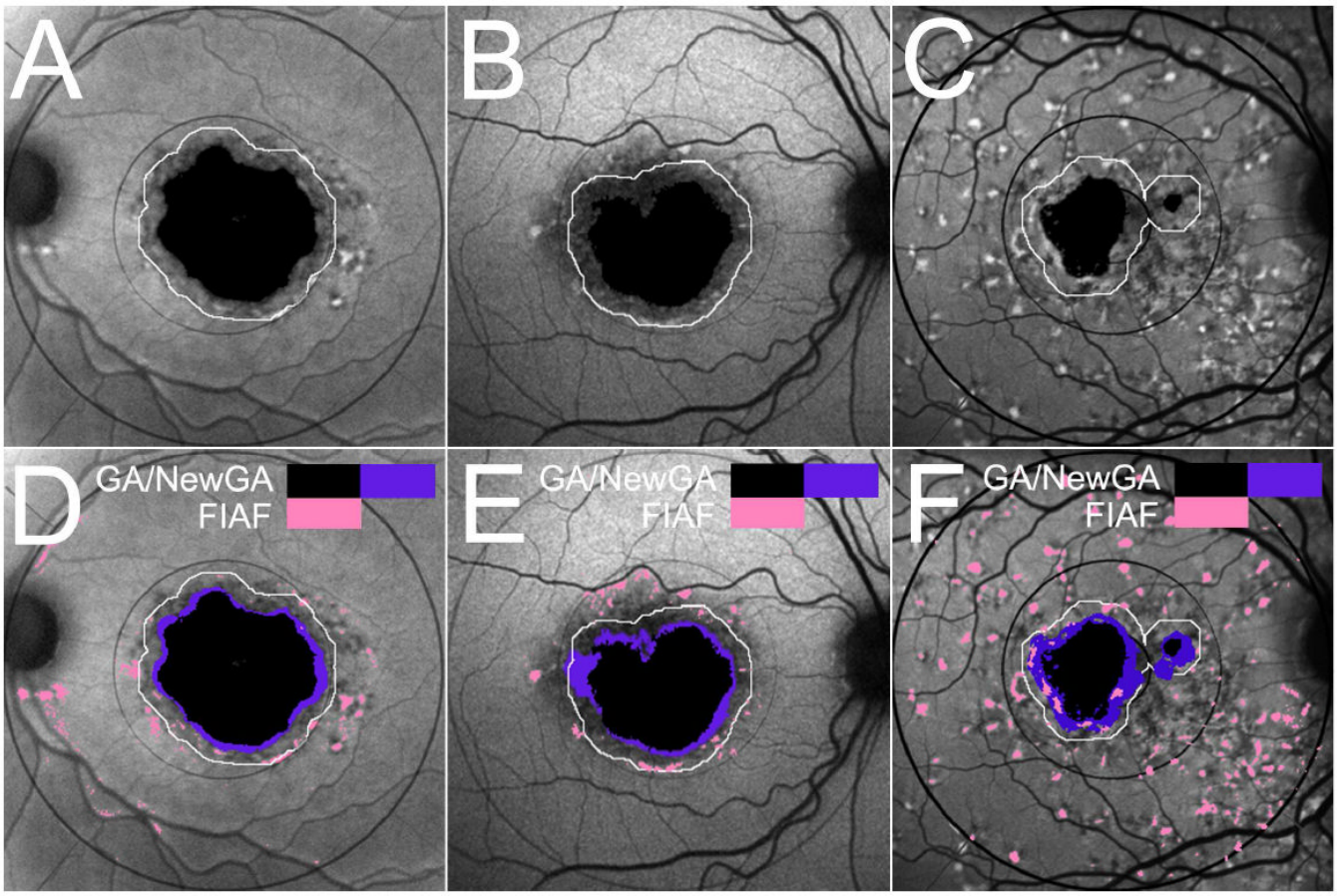

Fig 4. The three types of transition zone for geographic atrophy

A. Patient 3 OS, initial scan. The 250 μ transition zone has an essentially neutral AF level, similar to that of patient 2 OD (Fig 2), with patches of minimally elevated and decreased AF.

B. Patient 5 OD, initial scan. The transition zone is predominantly decreased autofluorescence.

C. Patient 10 OD, initial scan. The transition zone has mixed increased and decreased AF. Note that these three transition zones could simply represent progressive stages in the same basic process, with autofluorescence greatest in type **C**, neutral in type **A**, and least in type **B**.

D. Patient 3 OS, final scan, two year interval. New geographic atrophy (GA) is indicated in dark violet, and the FIAF from the *initial* scan in pink is superimposed, showing essentially no correspondence with the new GA. This result is also quite similar to that of patient 2 OD (Fig 2).

E. Patient 5 OD, final scan, one year interval. The relationship of initial FIAF and new GA is much like **D**.

F. Patient 10 OD, final scan, two year interval. The initial focally increased autofluorescence (FIAF) in the transition zone largely coincides with new GA, but there is also significant new GA nasally where no FIAF was present. In fact, in each of these cases the GA has grown uniformly circumferentially with no quadrantic preference.

Table 1

Predictive value of focally increased autofluorescence (FIAF) for progression of focally decreased autofluorescence (FDAF). Serial AF images were analyzed. Areas of FIAF were identified on the initial image and areas of FDAF were identified on the final image. Each was measured as a percentage of the region that included both on the registered final image. PPV_FIAF (positive predictive value) is the probability that pixels with FIAF in the initial image became part of new FDAF in the final image. NPV_FIAF (negative predictive value) is the probability that pixels without increased FAF did not become FDAF pixels.

Patient #	Eye	Age	Age of onset	Duration between AF images (years)	New FDAF (PPV_Chance)	FIAF	PPV_FIAF	NPV_Chance	NPV_FIAF	Change FIAF/Yr	Change FDAF/Yr
1	OD	52	50	1	3.4%	2.0%	3.1%	97%	97%	-31.2%	97.2%
	OS			1	4.6%	2.3%	0.4%	95%	95%	32.3%	-11.8%
2	OD	52	45	2	5.3%	1.8%	1.7%	95%	95%	7.2%	14.3%
	OS			2	7.7%	1.6%	4.8%	92%	92%	-13.3%	15.2%
3	OD	57	42	2	16.8%	3.1%	13.3%	83%	83%	4.5%	13.4%
	OS			2	5.9%	3.7%	5.5%	94%	94%	4.8%	-5.3%
4	OD	19	14	3	1.4%	1.6%	1.4%	99%	99%	6.2%	19.8%
	OS			3	1.0%	1.3%	0.9%	99%	99%	-8.8%	-8.4%
5	OD	45	29	1	4.9%	4.1%	2.7%	95%	95%	-53.2%	-51.2%
	OS			1	5.3%	3.2%	0.8%	95%	95%	-91.1%	31.5%
6	OD	7.6	6.0	1.6	10.1%	11.2%	1.8%	90%	89%	-42.8%	88.9%
	OS			1.6	4.4%	10.4%	0.4%	96%	95%	65.4%	-4.7%
7	OD	19	18	1	4.8%	2.5%	4.9%	95%	95%	-41.2%	46.4%
	OS			1	9.1%	4.2%	10.6%	91%	91%	-45.1%	72.3%
8	OD	30	21	5	7.1%	11.5%	4.8%	93%	86%	-12.9%	146.8%
	OS			5	14.6%	14.7%	14.5%	85%	85%	-5.8%	47.2%
9	OD	12	11	1	**	0.2%	*	**	*	*	10.2%
	OS			1	**	0.7%	*	**	*	*	8.2%
10	OD	44	30	2	7.8%	4.9%	5.7%	92%	92%	-26.9%	25.9%
	OS			2	5.6%	3.0%	0.6%	94%	94%	-31.8%	33.4%
MEAN		34	27	2.0	6.7%	4.4%	4.3%	93%	93%	-15.8%	29.5%
STDEV		18	15	1.3	4.0%	4.1%	4.4%	4.0%	4.1%	35.0%	44.7%

* FIAF amounts too small for meaningful calculation, but did give PPV of zero;

** omitted because FIAF too small for comparison of PPV.

Table 2

Predictive value of focally increased autofluorescence (FIAF) for junctional geographic atrophy (GA) progression. Serial AF images were analyzed for eyes with GA. Areas of GA were identified on the initial and final images. FIAF was identified and measured as a percentage of the 250 micron border zone surrounding the initial GA lesion. PPV_FIAF (positive predictive value) is the probability that pixels with FIAF in the initial image became part of new GA in the final image. NPV_FIAF (negative predictive value) is the probability that pixels without increased FAF did not become atrophic.

Patient #	Eye	Duration between images (years)	New GA (PPV_Chance)	FIAF	PPV_ FIAF	NPV_ Chance	NPV_FIAF	IncrGA/Yr
2	OD	2	24.8%	0.8%	0.0%	75.2%	75.0%	29.7%
2	OS	2	22.5%	3.2%	1.4%	77.5%	76.9%	13.8%
3	OD	2	32.0%	3.3%	20.7%	68.0%	67.6%	8.2%
3	OS	2	25.2%	2.1%	2.9%	74.8%	74.4%	8.7%
5	OD	1	27.0%	2.9%	0.0%	73.0%	72.2%	29.5%
10	OD	2	47.7%	9.6%	61.8%	52.3%	53.8%	43.7%
10	OS	2	49.5%	0.1%	0.0%	50.5%	50.5%	530.6%
MEAN		1.960	32.6%	3.1%	12.4%	67.4%	67.2%	*29.5%
STDEV		1.290	3.6%	1.0%	8.9%	3.6%	3.5%	N/A

*median value.

Table 3

Sensitivity of predictive value of focally increased autofluorescence (FIAF) for new focally decreased autofluorescence (FDAF) to standard deviation thresholds used to define FIAF and FDAF (four selected eyes of four patients); sensitivity of predictive value of FIAF for new geographic atrophy (GA) for one eye. Pixels were originally defined to have FIAF (FDAF) if their gray levels were greater than (less than) 1.5 standard deviations above (below) the leveled image mean. The threshold used to define FIAF/FDAF was varied from 1.0 to 2.0 standard deviations (SD) to measure the impact on predictive values. PPV_FIAF (positive predictive value) is the probability that pixels with FIAF in the initial image became part of new FDAF (or new GA) in the final image. NPV_FIAF (negative predictive value) is the probability that pixels without increased FAF did not become FDAF pixels (or become atrophic).

Patient #	Eye	SD	New FDAF (PPV_Chance)	FIAF	PPV_FI AF	NPV_ Chance	NPV_FI AF
		2	1.7%	0.8%	1.3%	98.3%	98.3%
1	OD	1.5	3.4%	1.8%	3.1%	96.6%	96.6%
		1	5.1%	1.9%	7.7%	94.9%	95.0%
		2	1.8%	0.8%	0.0%	98.2%	98.2%
4	OS	1.5	1.0%	1.3%	0.9%	99.0%	99.0%
		1	2.9%	2.7%	1.0%	97.1%	97.1%
		2	3.9%	3.4%	6.0%	96.1%	96.2%
7	OS	1.5	9.1%	4.2%	10.6%	90.9%	90.9%
		1	7.1%	14.5%	6.0%	92.9%	92.8%
		2	7.7%	4.2%	3.2%	92.3%	92.1%
10	OD_FDA F	1.5	7.8%	4.9%	5.7%	92.2%	92.1%
		1	5.6%	7.6%	4.4%	94.4%	94.3%
			New GA (PPV_Chance)				
		2	49.8%	5.0%	74.9%	50.2%	51.6%
10	OD_GA	1.5	47.7%	9.6%	61.8%	52.3%	53.8%
		1	49.7%	9.6%	63.2%	50.3%	51.7%